SLAC - PUB - 2040
NOVEMBER 1977
(T/E)

DIRECT ELECTRON PRODUCTION MEASUREMENTS BY DELCO[1] AT SPEAR†

Jasper Kirkby
Stanford Linear Accelerator Center and Physics Department
Stanford University, Stanford, California 94305

ABSTRACT

We have observed weakly-produced electrons in e^+e^- annihilations above $E_{c.m.} \sim 3.75$ GeV. In the course of a scan through this threshold region we observed the $^3D_1$ state of charmonium with a mass 3770 ± 6 MeV/c^2, width $\Gamma = 24 \pm 5$ MeV and partial width to electron pairs $\Gamma_{ee} = 180 \pm 60$ eV. This resonance (named $\psi''(3770)$) provides a value for the D semileptonic branching ratio of $11 \pm 3\%$. On the assumption of the Cabibbo nature involved, the ψ'' electron momentum spectrum indicates a substantial contribution from the mode $D \rightarrow Ke\nu$. A comparison of the events having only two visible prongs (of which only one is an electron) with the heavy lepton hypothesis shows no disagreement. Alternative hypotheses have not yet been investigated.

†Work supported by the U.S. National Science Foundation and the Dept. of Energy.

(Presented to 1977 International Symposium on Lepton and Photon Interactions at High Energies, Hamburg, Germany, August 25-31, 1977)

I INTRODUCTION

At the previous symposium at Stanford an enormous amount of data was presented barely a year after the J/ψ discovery. The e^+e^- annihilation experiments had uncovered a spectrum of C-even states in radiative decays of the ψ and ψ' and a rich resonance region separating two plateaus in the total hadronic cross section. The most compelling explanation for these results was a new quantum number, charm, but unfortunately there was no conclusive evidence. Indeed, there were even difficulties such as apparently no increase in charged kaon yield above E_{cm}=4 GeV and the exclusion of predicted D decay modes to the few percent level.

A result which appeared unrelated to, but no less remarkable than the emerging charm picture was the observation of anomalous e-μ events at SPEAR and their suggested interpretation as the decay products of a pair of heavy leptons. Since the lowest mass particles which carry a new quantum number must decay weakly and therefore semi-leptonically it was apparent that an important field of research was prompt lepton production in e^+e^- annihilations.

The size of the expected signal was reasonably large: the cross section for either charmed hadrons or heavy leptons is about 1 (R units i.e., relative to the point cross section) and the branching ratio to $e\nu X$ is about 10%. Since the total hadronic cross section is about 5, then it is expected that 4% of the hadronic events might involve weakly-produced electrons or alternatively they form 1% of the prongs. This is not a difficult experimental problem but the low lepton momentum (< 1 GeV/c) strongly favored the measurement of electrons in a gas Cerenkov counter (which can readily achieve 10^{-3} hadron rejection).

Such was the atmosphere two years ago which was molding the design of DELCO, and today I will report the first measurements by the detector.

II. APPARATUS

The performance of a Cerenkov counter is degraded by entrance material (which results in δ ray production and photon conversions). This characteristic led to a somewhat unconventional approach in the design of the magnetic detector as shown in Figs. 1a and 1b. The 3.5 kG analyzing field is approximately axial and is produced by two discrete coils wrapped on steel pole-pieces. By placement of the flux return yoke outside the detector there results an unobstructed path for particles emitted at angles greater than 40° with respect to the beam axis. The field volume is small, the field integral is 1.7 kGm, but the momentum accuracy due to measurement errors is 13 p(GeV)% when information in the outer magnetostrictive wire spark chambers (WSC) is included.

Tracks emerging from the luminous region, which extends ~2cm (σ) along the beam axis and transversely ~0.1 cm, leave a thin (0.015cm) stainless steel beam pipe and enter a set of 6 cylindrical multi-wire proportional chambers (MWPC). The solid angle subtended by the complete MWPC is 75% of 4π steradians and the inner two cylinders cover 90% of 4π str. Azimuthal readout is provided by axial anode wires of 2mm spacing and crude depth measurement by four cylindrical HV foils divided into 1 cm wide strips inclined at $\pm 45^{\circ}$ to the beam axis.

Immediately beyond the MWPC, the particles enter a 12-module ethane-filled Cerenkov counter sensitive only to electrons (π threshold = 3.7 GeV/c). Particles which count by striking the photocathodes are identified by plastic guard counters.

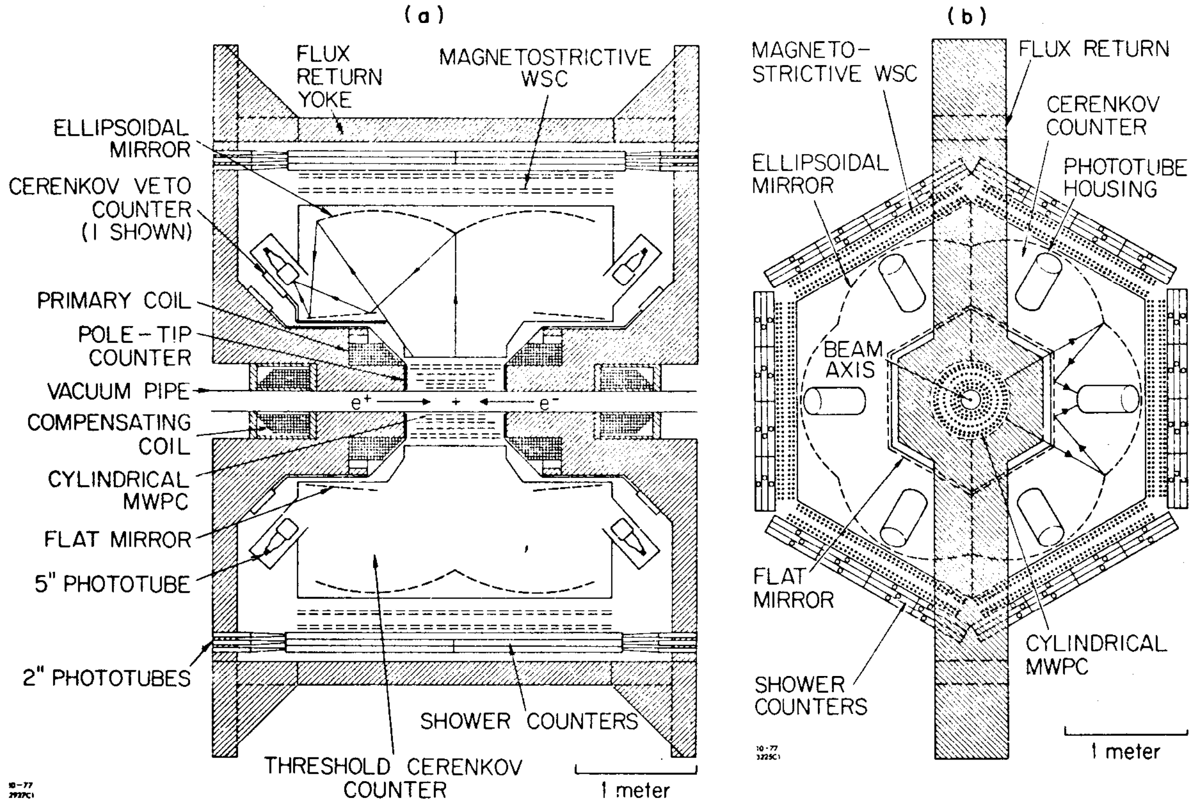

Figs. 1a and 1b. Polar (a) and azimuthal (b) projections of the apparatus.

Within each module, the Cerenkov light is focussed by a 1.4×1.4 m ellipsoidal mirror via a flat mirror onto a 5" RCA 4522 phototube coated with pTP wave-shifter. The counter provides an average radiator length of 1 m over 65% of 4π steradians and yields 10 photo-electrons for a β=1 particle.

Next in each sextant are located 2 WSC's providing a pair of z and ϕ measurements per track. Finally there is an array of Pb/scintillator shower counters subtending 60% of 4π steradians and consisting of 3 layers of Pb (2rl) and scintillator. The first layer of scintillator (A counter) is full length and is viewed at each end by a 2" phototube. The following layers are composed of two half-length scintillators, each viewed individually.

In addition, the region between 15° and 35° relative to the beam axis is covered by pie-shaped counters attached to the magnet pole tips and read out via blue → green wavelength shifter bars.

All the phototubes are pulse height analyzed and all but those on the outer two layers of the shower counters are also time analyzed.

III. TRIGGERS AND EVENT IDENTIFICATION

The apparatus is triggered by the coincidence of two shower counters (2S) from separate sextants and a track in the inner two MWPC planes occurring within 20 nsec of the beam cross-over time. The coincidence of at least 2 of the three scintillator layers forms 1S which is thereby satisfied by photons in addition to charged tracks. Two additional triggers which allow all-neutral final states are used, equivalent to

3S and 2S with a minimum pulse height restriction to exclude cosmic rays. The combined trigger rate is 0.7 H_z.

After track finding, cosmic events are removed on the basis of timing and vertex cuts. The remaining 15% or so of the triggers are classified as annihilation events:

a) Hadronic

b) Bhabha ($e^+e^- \longrightarrow e^+e^-$)

c) $e^+e^- \longrightarrow \mu^+\mu^-$

d) Other qed (e.g., $e^+e^-\gamma$, $e^+e^-e^+e^-$, $\gamma\gamma$ etc.)

e) Residue

The wide-angle Bhabha events are efficiently recognized by a combination of shower pulse height and Cerenkov signals. They are approximately twice as abundant as the hadronic events and after radiative corrections provide our determination of the integrated luminosity.

Hadronic triggers include those events with at least three tracks emerging from the interaction region and having at least two in-time shower counters. In addition, two-track events are included if the tracks are not both electrons and are acoplanar with the beam axis by at least 5^o. Hadronic events with one or zero prongs are presently placed in a residue class and will be analyzed in the future.

Candidates for hadronic events with an $e^\pm$ form that subset of these events in which one of the tracks traverses a Cerenkov cell and a shower counter and both of these give an in-time pulse. To reduce the background from Dalitz pairs, γ conversions and δ rays, events are not accepted into this sample if the $e^\pm$ track is accompanied by another track within $\Delta\phi$ = 15/P(GeV) mrads, where P is the momentum of the softer track. This cut has been measured to remove (15±5)% of real events.

A 'hadronic' event with an electron and having only two visible prongs must succeed more restrictive cuts to remove electron-pair background. Both tracks must be above 300 MeV/c momentum and lie away from the Cerenkov mirror edges so that an efficient positive identification of the electron and an efficient exclusion of the other track as an electron are made. In addition, an acoplanarity angle of at least 20^o with respect to the beam is required.

The data sample I will discuss is based on 12 weeks of data-taking between April and June 1977. It is displayed in Table I according to the event categories just described.

IV. HADRONIC CROSS SECTION

The hadronic triggering efficiency cannot be determined accurately since it depends on the physics we want to study but do not yet know in detail. Our present calculation has been to unfold the 'true' charged track and photon multiplicity distribution from that observed, on the assumption of no correlation between final state products. Once this is known, the overall triggering efficiency is readily obtained by appropriately weighing the different final state efficiencies. For events with at least 4 prongs it is above 90% and for 2-prong events it is (48±15)%. The overall triggering efficiency at $E_{c.m.}$ of 3.8 GeV is 0.85±0.1 where the error was determined by taking extreme input assumptions compatible with the data.

Table I

Data Sample (12 Weeks)

$E_{c.m.}$ (GeV)	Hadrons ($\times 10^3$)	$e^{\pm}$ + $\geq$ 2 prongs (MP electron events)	#$e^{\pm}$ + 1 prong (eX events)
ψ	42	160	1
3.6	0.5	0	0
ψ'	17	150	7
ψ''(3770)	29	600	68
3.80 → 4.23	26	550	53
4.24 → 4.27	6	90	16
4.28 → 4.99	20	470	47
5.0 → 7.4	14	310	37
Totals	155	2300	230

Note: The number of events refers to those surviving the cuts discussed in Section III.

Based on the observed number of hadronic and Bhabha events and the detection efficiencies discussed above, we display in Fig. 2 the hadronic cross section ratio R, in the range $3.6 < E_{c.m.} < 4.8$ GeV. The errors shown are statistical and the vertical scale may possess an overall systematic error of ±20%. This region is of particular interest because it includes the thresholds for both the lowest mass charmed particle D^0 and the proposed heavy lepton τ and covers the resonance region.

The general features of this plot are in reasonable agreement with those previously measured at SPEAR[2] and DORIS.[3] Combining all data, R seems to rise from 2.5 below the ψ' to a value between 4.5 and 5 at 4.8 GeV. Above the rapid rise in cross section at 3.9 GeV the summed data supports three broad resonances of approximate masses 4.03, 4.16 and 4.41 GeV/c^2. These do not appear distinct in the data of Fig. 2.

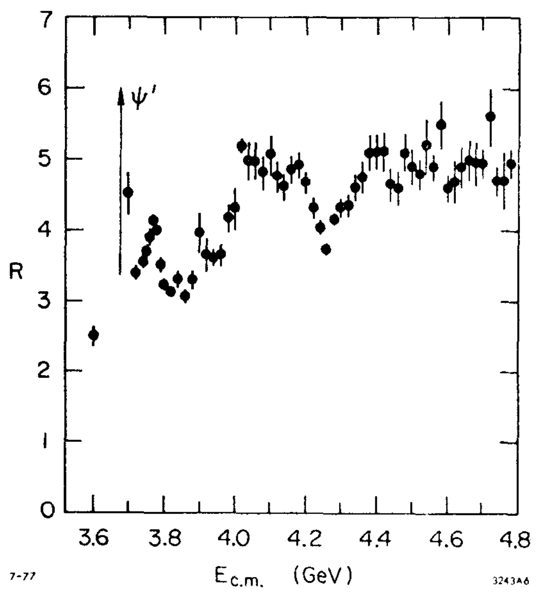

Fig. 2 The hadronic cross section $R = \sigma(e^+e^- \to \text{hadrons}) / \sigma(e^+e^- \to \mu^+\mu^-)$ as a function of center-of-mass energy.

V. ψ'' (3770) RESONANCE

In addition a new resonance has been observed[4] at 3.77 GeV in the course of our program to measure electron production close to D threshold. This is identified as the first $^3D_1$ state of charmonium with $J^{PC} = 1^{--}$ predicted in 1975 by Eichten et al.,[5] at this mass. It is somewhat of an experimental embarrassment that this distinct peak remained hidden for so long after such careful theoretical guidance. However, there existed uncertainty in the strength of the coupling between the photon and the $^3D_1$ state since its wave function at the origin is expected to vanish and it therefore can only be produced by mixing with the 2^3S_1 (ψ') state.

The value of R in the range 3.7 GeV $< E_{c.m.} <$ 3.83 GeV is displayed in Fig. 3a) and the same data after removal of the ψ and ψ' tails[6] is shown in Fig. 3b). We assume that $D\overline{D}$ is almost the entire decay mode of this new resonance (which is named the ψ''). This follows since the ψ' and ψ'' are separated in mass by less than 100 MeV and yet the latter, which lies above the DD thresholds,[7] has a width two orders of magnitude greater than the ψ'. We therefore tried several Breit-Wigner fits with and without dependencies on the momenta p_0 and p_+ of the D^0 and D^+ respectively. Specifically we used:

$$R = \frac{3\pi}{\sigma_{\mu\mu} m^2} \frac{\Gamma_{ee}\Gamma(E)}{(E_{c.m.} - m)^2 + \Gamma^2(E)/4} \qquad (1)$$

with

$$\Gamma(E) = \text{constant} \quad (\text{s - wave})$$

or

$$\Gamma(E) \propto \frac{p_0^{\,3}}{1 + (rp_0)^2} + \frac{p_+^{\,3}}{1 + (rp_+)^2} \quad (\text{p-wave}) \qquad (2)$$

where r represents an interaction radius.[8] The non-resonant background term was either linear or proportional to $(p_0^3 + p_+^3)$. All of these gave resonance parameters which agreed within the errors of the fits. Specifically, a p-wave final state with a $(p_0^3 + p_+^3)$ background gave: $m = (3770 \pm 6)$ MeV/c^2 (allowing for the energy calibration of SPEAR, $\Gamma = (24 \pm 5)$ MeV, $\Gamma_{ee} = (180 \pm 60)$ eV. The error in Γ_{ee} includes ± 40 eV due to the fit and ± 40 eV due to normalization uncertainties. Our values of m and Γ agree with those of Rapidis et al.[4] while our value of Γ_{ee} is less than theirs by a factor of two. Most of the discrepancy (a factor of 1.5) is accounted for by a difference in the raw data and an additional 20% is caused by uncertainties in normalization.

VI. MULTI-PRONG ELECTRONIC CROSS SECTION

Fig. 3c) displays the cross section ratio R_e where,

$$R_e = \frac{(e^+e^- \rightarrow \text{hadrons} + \geq 1 \text{ electron})}{(e^+e^- \rightarrow \mu^+\mu^-)}$$

with the requirement that at least two tracks (prongs) are visible in addition to the electron.[9] This is a historical cut which has been used to separate electron events from the two sources, charmed hadrons and heavy leptons. The expectation is that electrons from charm decays originate mainly in events containing four or more prongs and that electrons from heavy lepton decays originate mainly in two prong events. However, it should be stressed that in both cases 'mainly' is $\gtrsim 80\%$ and the separation is not complete. This will be discussed in more detail later. The data of Fig. 3c) has been corrected for all detection efficiencies with the exception of losses due to events which appear with two or less prongs. These result from both original two prong events and multi-prong events with unidentified tracks.

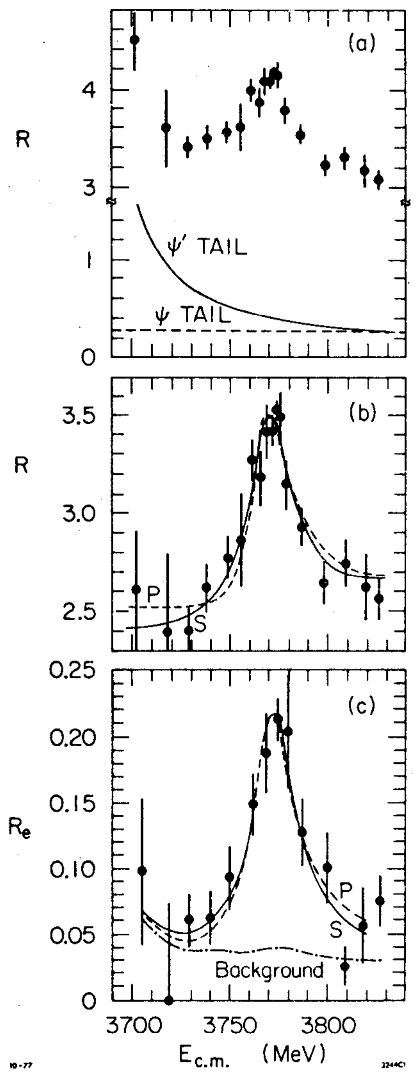

Fig. 3 a) R as a function of energy
b) R after subtraction of the radiative tails of ψ and ψ'
c) Re as a function of energy. The curves are described in the text.

An unmistakable peak in R_e is observed possessing the same mass and width as the ψ''. This provides unambiguous evidence for the semi-leptonic decays of D's. The dot-dash line is an absolute estimate of the background based on the assumption that there is no anomalous electron production at the ψ or ψ' and derived from the measured probability of observing an electron per hadronic event of $(3.5\pm0.3)\,10^{-3}$ at the ψ and $(8.8\pm1.0)\,10^{-3}$ at the ψ'. At the ψ' the observed rate is due mainly to $\psi \rightarrow \psi\pi^+\pi^- \rightarrow e^+e^-\,\pi^+\pi^-$ decays. At $E_{c.m.} = 3.6$ GeV no anomalous electrons were seen in a sample of 470 hadronic events, consistent with the rate measured at the ψ.

The multi-prong electron cross-section R_e is shown in Fig. 4 over a larger energy range,

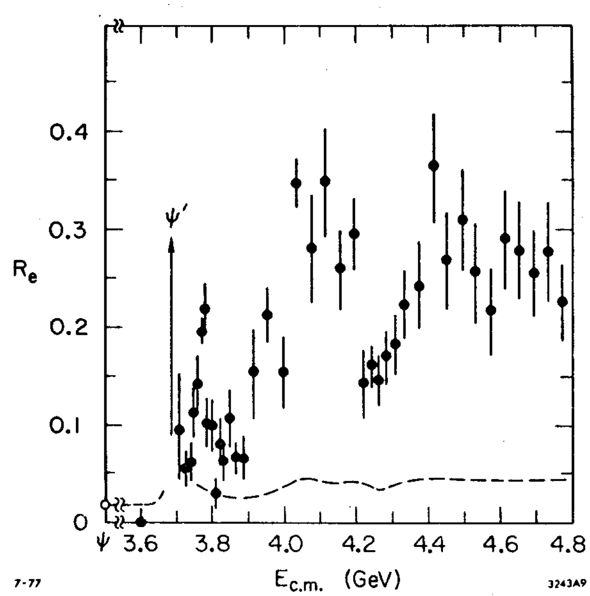

Fig. 4 Re over the energy range $3.6 < E_{c.m.} < 4.8$ GeV. The hollow point at the ψ is the quantity Re (ψ) x R $(3.6)/$ R (ψ). This point is used in the estimate of background as indicated by the dashed line.

$3.6 < E_{c.m.} < 4.8$ GeV. This data is a 'second generation' R measurement which provides a sensitive indicator ('charmometer') for charm production. The steep (60%) rise observed in the hadronic cross section at 4 GeV is seen even more dramatically in Fig. 4 where the electronic cross section is a factor of seven higher than the background. We also observe a region of very low electron production centered at $E_{c.m.} = 4.25$ GeV. Since it coincides with the dip observed in the hadron cross section (Fig. 2) we do not interpret this as the threshold of a new charmed hadron with a decreased semi-leptonic branching ratio. The importance of this region lies in allowing a study of the proposed heavy lepton decays under low charm background conditions.

Beyond $E_{c.m.} = 4.1$ GeV there are potential contributions from F semileptonic decays e.g., $\eta e\nu$ and $\phi e\nu$ and beyond 4.5 GeV charmed baryons may contribute via decays such as $\Lambda_c \to \Lambda e\nu$. At present we have made no attempt to isolate these components and the discussion in the next section will be limited to the events below $E_{c.m.} = 4.08$ GeV where the only charmed contribution is from D's.

VII. D SEMILEPTONIC DECAYS

A. Branching Ratio Measurements

The observation of the ψ'' resonance has provided a 'clean' laboratory, containing pure $D\bar{D}$ final states, for measuring detailed properties of D decays. On the assumption that the ψ'' has definite isospin, either 0 or 1, the relative $D^0\bar{D}^0$ and D^+D^- decay branching ratios are determined simply by the available phase space (Eq. 2). This implies a branching ratio of $(56\pm3)\%$ for the $\psi'' \to D^0\bar{D}^0$ and $(44\pm3)\%$ for $\psi'' \to D^+D^-$. However, for the present analysis we will assume that the total D^0 semileptonic and D^+ semileptonic branching ratios are equal, thereby we are insensitive to the exact mixture in the ψ'' decays.

There are two techniques for determining the ratio,

$$B = \frac{D \to e\nu\ X}{D\ \to ALL}$$

at the ψ'':

i) Comparison of the areas under the Breit-Wigner curves (Fig. 3)

ii) Comparison of the number of 1-electron events with those having 2 electrons.

Both techniques require a correction due to losses of D semileptonic decays into two-prong and lower classes. We have estimated this loss under the following assumptions:

i) D^0 decay prong distribution[7] is OP :2P:4P = 10%:70%:20%

ii) D^+ decay prong distribution[7] is 1P:3P = 40%:60%

iii) D^0 semileptonic decay prong distribution is 2P:4P = 90%:10%

iv) D^+ semileptonic decay prong distribution is 1P:3P = 45%:60%

v) No correlation between prongs

vi) Probability of missing a prong = 20%

vii) Equal production of charged and neutral D's at the ψ''. The calculation is insensitive to the expected deviation from this assumption.

Assumptions iii) and iv) appear reasonable in the light of the observed electron momenta and the observed prong distribution for 2-electron multiprong events shown in Table II.

Table II

Prong Distribution

of the 2-Electron Events at the ψ''

	Number of Detected Prongs			
	3	4	5	6
Observed	6	10	2	0
Predicted (according to the assumptions discussed in Section VII)	4	10	2	2

The results of the determination are summarized in Table III. It should be noted that this calculation of two-prong feed-down is only capable of providing a crude

Table III

Calculation of D Semileptonic Prong

Distributions at the ψ''

	Number of Prongs		
	1	2	MP($\geq$3)
a) For events containing at least one detected electron			
Original distribution	0	.13	.87
Detected distribution	(.03)	.16*	.81
b) For events containing at least two detected electrons			
Original distribution	0	.10	.90
Detected distribution	0	.13	.87

*The predicted 2P fraction 0.16 comprises 0.11 from events which were originally 2P and 0.05 from $\geq$4P events which were fed-down.

estimate with an error of ±50%. The most significant prediction is that 16% of the semileptonic events at the ψ'' should appear as 2 prongs in the final state. This will be important in the discussion of the heavy lepton events in the next section.

We are now in a position to determine the ratio B:

i) The ratio of the areas under the Breit-Wigner curves of Fig. 3 is 0.176±0.015 where the error is only statistical. From Table III we see this represents an estimated 81% of the total semileptonic decays. The branching ratio is then

$$B = \frac{1}{2} \times \frac{0.176}{0.81} = (11 \pm 3)\%$$

The error is dominated by uncertainties in the two-prong losses and by electron detection efficiencies. When these are better understood this technique should provide the best measurement since it measures a resonant component and is thereby insensitive to smooth backgrounds such as those from a potential heavy lepton.

ii) The number of 1-electron events (N_1) observed at the ψ'' and the number of 2-electron events (N_2) are used in the second determination of B:

$$B = \frac{2N_2/P_2 \times E}{N_1/P_1} ,$$

where $P_1(P_2)$ is a probability that a 1- (2-) electron event will appear as a multiprong given 1 (2) electrons inside the detector and E is the electron detection efficiency. The value of E is 0.39, resulting from losses due to solid angle, low momentum electrons and software. The ratio P_1/P_2 is .81/.87 = 0.93 as seen from Table III. The number of observed 1-electron events is 596 of which an estimated 20% are background. The number of 2-electron events is 18 (after removal of $\psi' \to \psi\pi^+\pi^- \to e^+e^-\pi^+\pi^-$ decays) of which we estimate 2 are background due to misidentification of one electron. The branching ratio is then:

$$B = 2 \times \frac{16}{596 \times 0.8} \times \frac{0.93}{0.39} = (16 \pm 4)\%$$

where the error quoted is statistical only. This measurement should only be considered as a consistency check on the previous value. We have not yet eliminated processes such as residual wide-angle Dalitz pairs and 2-photon events which may contribute to N_2 and thereby systematically increase the measurement of B.

A total D semileptonic branching ratio of (11±3)% supports the existence of an enhancement of the calculated non-leptonic decay rates similar in strength to that found necessary for K decays. The latter is the empirical '$\Delta I = 1/2$ rule' for which several mechanisms have been suggested.[10]

It is possible to measure separately the branching ratios $D^0 \to e\nu X$ and $D^+ \to e\nu X$ by comparing the inclusive electron production at the ψ'' and at $E_{c.m.} = 4.03$ GeV. As input one needs the relative production cross sections[7] ($\sigma_{4.03}/\sigma_{\psi''}$) for D^0's (2.4±0.5) and D^+'s (1.2±0.3). This increase in D production by almost a factor of 2 is not reflected in the semileptonic data (Fig. 4) which suggests a smaller increase of perhaps 50% in cross-section. The inference is that the D^+ semileptonic branching ratio is larger than that of the D^0 since the latter particle is responsible for most of the increase in charm cross section at $E_{c.m.} = 4.03$ GeV. The errors involved in this calculation at present preclude other than these qualitative considerations.

B. Electron Momentum Spectra.

The expected semileptonic decay modes of D's and the appropriate selection rules are readily seen in the quark diagrams of Fig. 5:

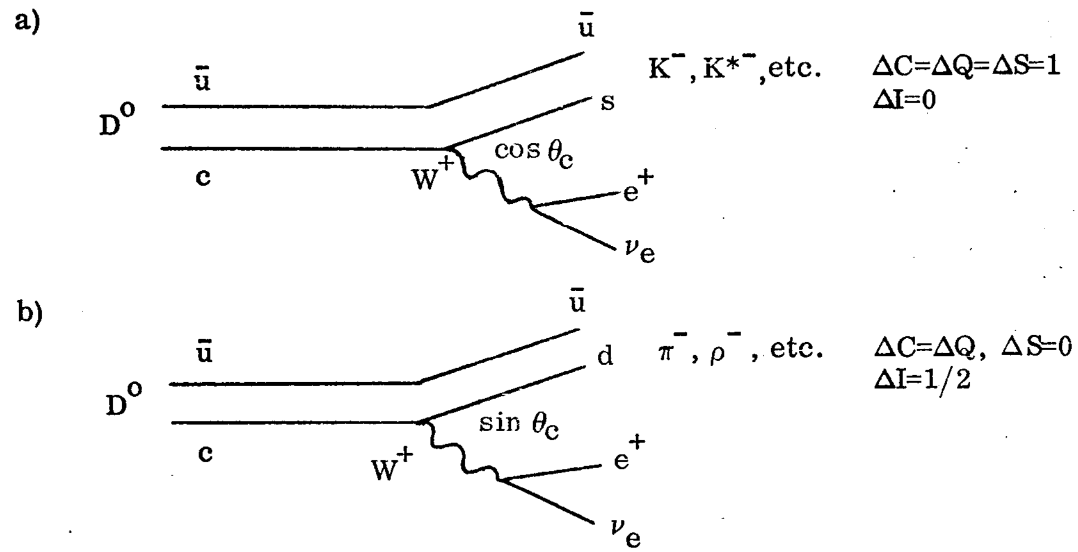

Fig. 5 Cabibbo favored a) and suppressed b) semileptonic decay modes of D^0.

The general expectation in the extensive literature[11] on this subject is that among the Cabibbo-favored decays, the dominant should be $D \rightarrow Ke\nu$ and $D \rightarrow K^*(890)\, e\nu$. Phase-space is expected to inhibit the decay into K^{**} (1420) and soft pion theories suppress non-resonant $K\, n\pi$ production.

The simplest experimental parameter to separate the decay modes is the electron momentum spectrum. This is shown in Fig. 6 for the multiprong electrons at the ψ''. This data has been subjected to restrictive cuts to ensure a clean, well measured, electron sample; e.g., only full-field data is included and events were not allowed if the electron and another track entered the same Cerenkov cell. In addition, events were removed if they possessed two electrons consistent with the cascade decay

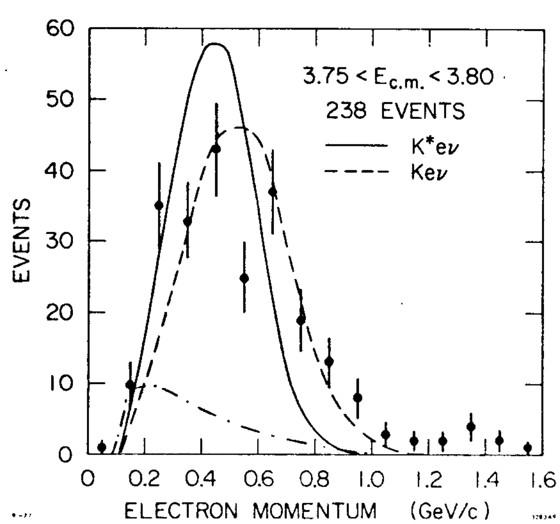

Fig. 6 Electron momentum spectrum for the multiprong events at the ψ''. The dashed and solid curves show the expected shapes for the decay modes $D \rightarrow Ke\nu$ and $D \rightarrow K^*e\nu$ (V-A) respectively. The dot-dash curve indicates the estimated background remaining in the data.

$\psi' \rightarrow \psi\,\pi^+\pi^-$ followed by $\psi \rightarrow e^+e^-$. This removal is not complete since occasionally one of the two electrons is undetected. The lepton spectra are obtained from the second paper of reference[11] and have been modified to account for momentum resolution and the Cerenkov detection efficiency of Fig. 7. This curve includes losses due to mirror edges and illustrates the effect of poor light collection below 0.2 GeV/c momentum.

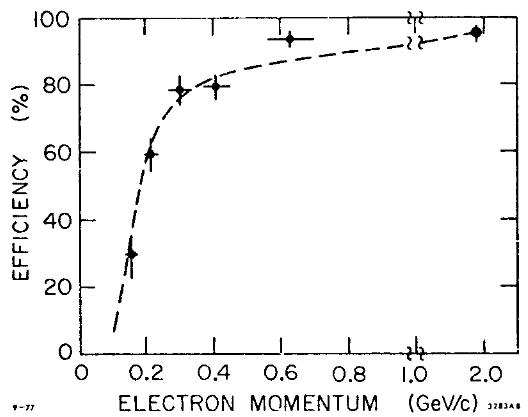

Fig. 7 Cerenkov detection efficiency as a function of electron momentum. The dashed line is the Monte-Carlo prediction and the data points are derived from the reactions $e^+e^- \rightarrow e^+e^-\,e^+e^-$ (at low momentum) and $e^+e^- \rightarrow e^+e^-$ (at high momentum).

We have verified our understanding of momentum measurements, particularly with regard to 'tails' by a study (as yet incomplete) of pion, dimuon and Bhabha momenta. With the caveat that we have assumed the Cabibbo nature involved, the data of Fig. 6 indicates that the decay $D \rightarrow Ke\nu$ is necessary to accommodate the higher momentum events we observe. (This data can contain a negligible small contribution from the proposed heavy lepton due to the phase space factor suppression). This conclusion is also obtained from the electron spectra above the ψ'' in the range $3.8 < E_{c.m.} < 4.08$ GeV as seen in Fig. 8.

We have also taken data at the ψ'' with the magnetic field at half strength and this allows sensitivity to the electrons from the process $D \rightarrow K^{**}(1420)e\nu$. These electrons peak at a momentum of 200 MeV/c and so the measurement is quite sensitive to the quality of understanding of the low momentum Cerenkov efficiency. With this disclaimer we find that the mode $K^{**}(1420)e\nu$ is less than 10% (90% CL) of the total semileptonic decay rate.

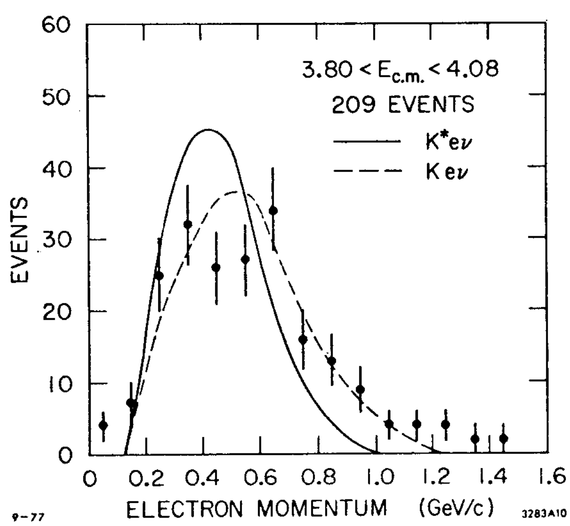

Fig. 8 Electron momentum spectrum for the multiprong events in the energy range $3.80 < E_{c.m.} < 4.08$ GeV.

In order to separate the decay modes and indeed to measure their Cabibbo nature it will be necessary to make a detailed study of the particles associated with the electron. For example, the K from $Ke\nu$ decay has a substantially higher momentum than that from $K^*e\nu$ decay. This separation is important since the decay $K^*e\nu$ measures the V, A nature of the weak current in charm semileptonic decays.

VIII. TWO-PRONG ELECTRON EVENTS

A. Comparison With the τ Hypothesis

We have isolated a sample of events containing only two visible prongs (with $\geq 0\gamma$'s) of which one is an electron and the other not an electron (as discussed in Section III and listed in Table I). The tracks are identified simply by the absence or presence of an in-time

Cerenkov latch; therefore, the observed shower pulse-heights (Fig. 9) provide an independent check of the nature of the tracks. The solid line of Fig. 9 corresponds

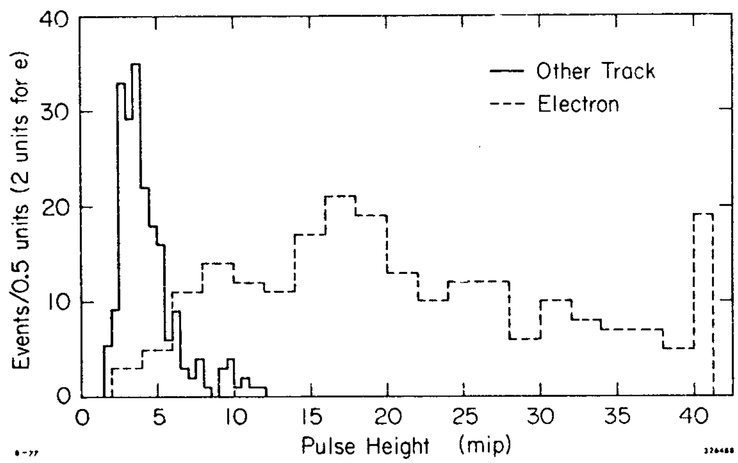

Fig. 9 Shower pulse height distributions for the two-prong (eX) events.

to the pulse height distribution expected from minimum ionizing particles and indicates, with further considerations, a background of $\leq 1\%$ from misidentified e^+e^- events.

This class of events has been observed by other e^+e^- experiments[12,3] which interpret their origin as the heavy lepton pair, $\tau^+\tau^-$. Accordingly we have compared our data sample with a sequential heavy lepton whose characteristics are listed in Table IV. The conclusion drawn from the data about to be presented is that it is not inconsistent with the τ hypothesis. This does not imply the conclusion that the data requires the heavy lepton. The latter question can only be addressed after more detailed analysis particularly with respect to the charm contribution to these events.

The production cross section ratio of the two-prong electron events is shown in Fig. 10. The hollow point at the ψ is the quantity $r_e(\psi) \times R(3.6)/R(\psi)$ and indicates a negligible background from noncharm hadronic events.

The vertical scale has an uncertainty of $\pm 50\%$ due to incomplete knowledge of acceptance. The curve shows the expected smooth yield from a heavy lepton pair with a branching ratio of 0.15 to $\nu_\tau e^- \bar{\nu}_e$. Here we have assumed that the relative rates of the decay modes listed in Table IV are well known with the exception of the ν_τ-hadron continuum mode. Hence a suppression of the branching ratio to $\nu_\tau e^- \bar{\nu}_e$ requires a suppression by the same factor of all modes except that of the hadron continuum. The data has been binned to allow maximum sensitivity to the variations in charm production cross section observed in the multiprong electron events. The latter are displayed for comparison on the same scale in Fig. 11. The curve follows the structure indicated by the data of Fig. 4. (The data above $E_{c.m.} = 5$ GeV may possess backgrounds not present at lower energies and therefore the apparent rise in Re at high energy cannot be considered significant).

The following points emerge in the comparison of Figs. 10 and 11:

i) Significant structure appears in the two-prong data at the ψ''.

ii) The multiprong cross section falls by more than a factor of two between

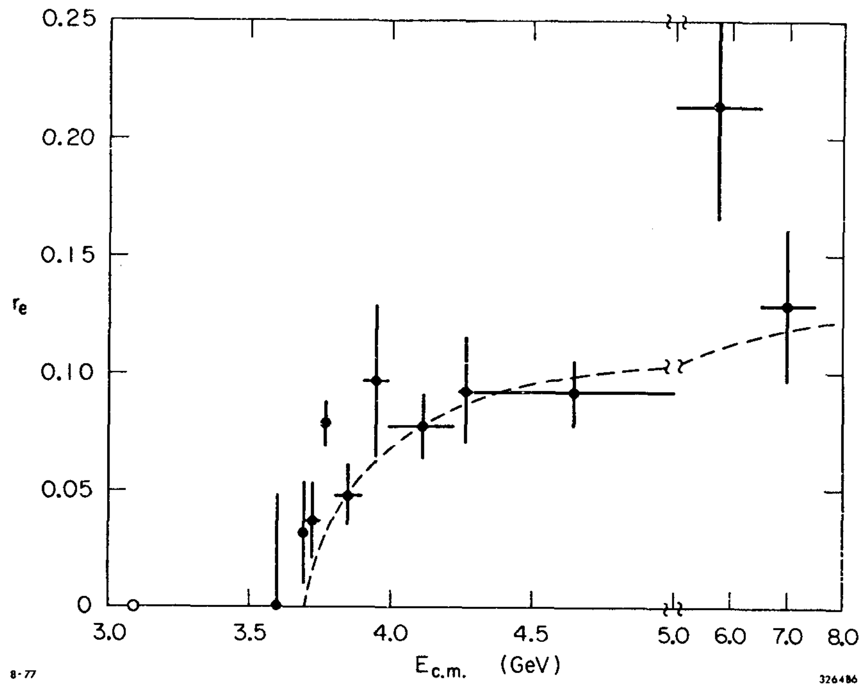

Fig. 10 The two-prong electronic cross section ratio $r_e = \sigma(e^+e^- \to eX + \geq 0\gamma\text{'s})/\sigma(e^+e^- \to \mu^+\mu^-)$ as a function of center-of-mass energy. The curve shows the expected yield from $\tau^+\tau^-$ as discussed in the text.

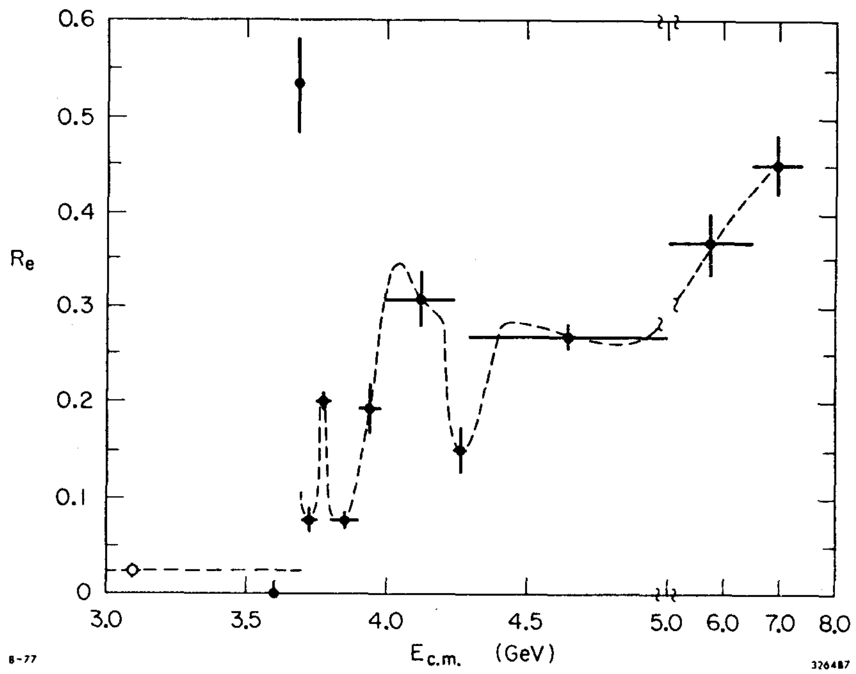

Fig. 11 Re as a function of center-of-mass energy. The curve follows the same data when displayed on a finer scale.

Tabie IV

τ Characteristics Assumed for Comparison With Data

i)	Mass = 1.85 GeV/c^2	
ii)	V-A Coupling	
iii)	Branching ratios:	Mode:
	0.20	$\nu_\tau\ e^-\bar{\nu}_e$
	0.20	$\nu_\tau\ \mu^-\bar{\nu}\mu$
	0.11	$\nu_\tau\ \pi^-$
	0.01	$\nu_\tau\ K^-$
	0.22	$\nu_\tau\ \rho^-$
	0.01	$\nu_\tau\ K^{*-}$
	0.07	$\nu_\tau\ A_1^-$
	0.18	ν_τ hadron continuum

$E_{c.m.}$ = 4.0 - 4.2 GeV and $E_{c.m.}$ =4.25 GeV. This decrease is not suggested in the two-prong data.

iii) The two-prong cross section does not decrease at the highest energies.

We have estimated the expected two-prong contribution from $D\bar{D}$ decays at the ψ'' according to the assumptions described in the previous section. From Table III we expected 0.16 of the semileptonic decays to appear as two-prongs and 0.81 to appear as multiprongs. So from the (596) observed multiprong events we determine 0.16 x 596/0.81 = 118 events will be contributed to the two-prong sample. This class is subject to additional cuts such as a minimum momentum for each track of 300 MeV/c and an acolinearity cut of $\Delta\phi < 160^o$. Their effect has been calculated from the multiprong sample and the net attenuation is by a factor 0.21 to yield a final contribution of 0.21 x 118 = 24 events. This is to be compared with the 68 events observed, i.e., approximately one third may be from $D\bar{D}$ decays. The calculation indicates that the ψ'' structure in the two-prong data is compatible with $D\bar{D}$ feed in.

It is clearly of great importance to improve this calculation and to apply the correction at all beam energies. This has not yet been carried out. We expect it to be a substantial correction for slow D*'s due to the difficulty in observing the soft π in the decay to D's.

We show the electron momentum distribution in Fig. 12 for the two-prong events in the range $3.8 < E_{c.m.} < 5.0$ GeV. The shape agrees with that expected from τ decay as indicated by the curve. We also plot the acolinearity angle $\Delta\phi$, defined in

Fig. 13. The curves show peaking at higher energies characteristic of production of the electron and the X particle by separate parents.

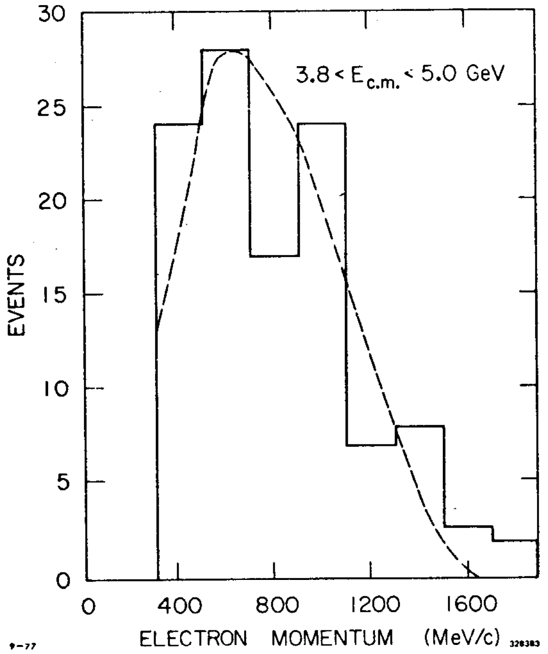

Fig. 12 Electron momentum of the two-prong electron events.

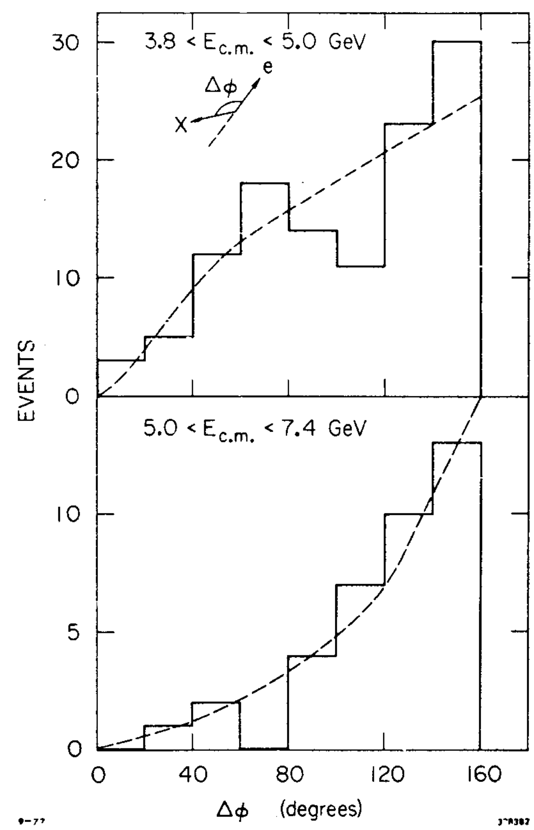

Fig. 13 Acolinearity angle, $\Delta\phi$, of the two-prong electron events for two $E_{c.m.}$ regions.

B. The Charm Question

The existence of anomalous $e\mu$, μX and eX events in e^+e^- annihilation is well established.[12] Furthermore these events have been found to be consistent with the decay products of a sequential heavy lepton τ. However, since the threshold of these events is close to that of charmed particles which are known to decay into leptons it is crucial that this interpretation of their origin is eliminated.

We will briefly list the arguments which have been made against the charm hypothesis and include some qualifications:

i) The cross sections are pointlike. However, no data can rule out the charm structure indicated by Fig. 11. Furthermore, at higher energies it has been assumed that charmed particles are produced in higher multiplicity final states thereby reducing the probability of a two-prong final state. This should be experimentally established.

ii) There exists a large signal of $e\mu$ events with no other observed particle. This places strong constraints on a charm origin. It implies a decay $\ell\nu$ + neutral where arguments have been given against the neutral being photons or a K_L^0 in the majority of the events. A candidate source at higher energies is $F^{*+} \rightarrow e^+ \nu_e$.

iii) The momentum spectra of the leptons are hard, unlike the spectra observed in charm decays. Here there is a kinematic bias away from high multiplicity (low lepton momentum) charm decays. Additionally there may exist a small rate of two-body leptonic decays which distorts the spectrum by contributing high energy leptons.

iv) The association with charged kaons is small. DASP measures[3] the probability of 0.07 ± 0.06 for the particle accompanying an electron in the two-prong events to be a $K^{\pm}$. This is compared with a fraction 0.24 ± 0.05 of $K^{\pm}$ per prong in the multiprong electron data. If one takes the picture suggested by ii) then the electron is accompanied by neutrals and only the other particle may generate a $K^{\pm}$. Then the comparison is made with the fraction $0.5 x (0.24 \pm 0.05)$.

We believe that an unambiguous dissociation of charm as the origin of the two-prong lepton events is best accomplished by a detailed comparison with the multiprong electron events through the full center-of-mass range. This covers the thresholds of several charmed particles each with different and perhaps unexpected decays into leptons which might result in a complicated composite origin of the two-prong leptonic events.

ACKNOWLEDGMENTS

It is a pleasure to thank A. Baumgarten, L. Birkwood, M. Chronoviat, R. Coombes, D. Ouimette, K. Porzuczek, D. Porat and C. Rasmussen for their outstanding contributions to the construction of this detector. I would also like to thank the SLAC Experimental Facilities Division and the SPEAR Operation Group for their splendid support of the experiment.

REFERENCES*

1. The experimenters involved with DELCO (an acronym of Direct Electron Counter) are: W. Bacino, C. Buchanon, R. Burns, P. Condon, P. Cowell, A. Diamant-Berger, M. Faessler, T. Ferguson, A. Hall, J. Hauptman, J. Kirkby, J. Kirz, J. Liu, L. Nodulman, M. Schwartz, W. Slater, H. Ticho, S. Wojcicki and C. Zupancic. SLAC, Stanford University, University of California Los Angeles and University of California, Irvine.

2. J. Siegrist et al., Phys. Rev. Lett. 36, 700 (1976).

3. The latest results are presented at this conference by A. Barbaro-Galtieri, (Pb-Glass Wall Collaboration: LBL, SLAC, Hawaii, Northwestern, Stanford), G. Knies (PLUTO Collaboration: DESY, Aachen, Hamburg, Siegen, Wuppertal), and S. Yamada (DASP Collaboration: DESY, RWTH Aachen, Hamburg, MPI Munich, Tokyo).

4. A parallel observation of this structure has been made at the SPEAR west interaction region. P. Rapidis et al., Phys. Rev. Lett. 39, 526 (1977).

5. E. Eichten et al., Phys. Rev. Lett. 34, 369 (1975), K. Lane and E. Eichten, Phys. Rev. Lett. 37, 477 (1976). See also K. Gottfreid in these proceedings.

6. J. Jackson and D. Scharre, Nucl. Inst. and Meth. 128, 13 (1975).

7. The $D^0\bar{D}^0$ threshold is (3726.6±1.8) MeV and the D^+D^- threshold is (3736.8±1.8). G. Feldman, SLAC Summer Institute on Particle Physics (1977).

8. J. Jackson, Nuovo Cimento 34, 1645 (1964), A. Barbaro-Galtieri, Advances in Particle Physics (Wiley, New York). Vol. II, 1968.

9. Such events were first observed by W. Braunschweg et al., Phys. Lett. 63B, 471 (1976).

10. J. Jackson. SLAC Summer Institute on Particle Physics, SLAC 198, 147 (1976). J. Ellis et al., Nucl. Phys. B100, 313 (1975).

11. The reader is referred to the following papers and references contained therein: M. Gaillard, B. Lee and J. Rosner, Rev. Mod. Phys. 47, 277 (1975), I. Hinchliffe and C. Llewellyn Smith, Nucl. Phys. B114, 45 (1976), A. Ali and T. Yang, Phys. Lett. 65B, 275 (1976), V. Barger, T. Gottschalk and R. Phillips, Phys. Rev. D, 16, 746 (1977), F. Bletzacker, H. Nieh and A. Soni, Phys. Rev. D. 16, 732 (1977), W. Wilson, Phys. Rev. D 16, 742 (1977). See also T. Walsh in these proceedings.

12. References are given by M. Perl in these proceedings.

*References to 'these proceedings' implies the 1977 International Symposium on Lepton and Photon Interactions at High Energies, Hamburg (August 1977).